Influence of Space Variant Effect on Axial Error in Digital Holography

Hao Yan, Chao Ping Chen**, Yikai Su***

*Department of Instrument Science and Engineering, School of Electronic Information and Electrical Engineering, Shanghai Jiao Tong University, Shanghai 200240, China

**National Engineering Lab for TFT-LCD Materials and Technologies, Department of Electronic Engineering, Shanghai Jiao Tong University, Shanghai 200240, China

Abstract

Digital holography (DH) is a 3D imaging technique with a theoretical axial resolution of better than 1-2 nm. However, practically, the axial resolution has been quoted to be in the range 10-20 nm. One possible reason is that the axial error is much larger so that the theoretical axial resolution cannot be achieved. The contributors to the axial errors of DH system need to be identified in order to reduce the errors. In this paper, the influence of space variant effect on the axial error is investigated by both simulation and experiment. The results show that space variant effect relates to the axial error. Position further away from optical axis suffers severer axial error. Asymmetrical displacement of object causes asymmetrical axial error. Therefore, objects are suggested to be placed on the optical axis and symmetrically for a better axial accuracy.

Keywords

digital holography; axial resolution; space variant; axial error

1. Objective and Background

Digital holography (DH) [1-2] is a 3D measurement and imaging technique. The recorded digital hologram is also applied in holographic display technique for optical 3D image reconstruction. The resolution of the 3D image is the key performance parameter in both DH and holographic display techniques. One of the advantages of holography over other 3D imaging techniques is its excellent axial imaging capability down to nanometer scale. This is because that, the imaging mechanism of holography in axial direction is based on the recording of the optical path differences (OPD) (OPD is obtained from the phase with OPD=phase/(2π)×wavelength), which is not affected by the diffraction limit. The impact of quantization effect on the axial imaging has been studied [3], which shows the axial resolution of 1-2 nm or less depending on the quantization bit numbers. However, in practical applications, such axial resolution is hard to achieve. The practical OPD resolution is usually in the range of 20-30 nm [2, 4]. One possible reason is that the axial error is much larger than the theoretical axial resolution. Tens of nanometers magnitude of axial error in DH has been reported by researchers [5-9]. Such axial error not only hinders the achievement of the theoretical axial resolution, but also affects the imaging accuracy, especially for objects with less than 100nm axial dimensions. Therefore the investigation of the axial error becomes necessary. However, the axial error has not been thoroughly investigated. In reference [10], it is found that CCD size relates to the axial error. Other contributors to the axial error also exist. Further investigations proceed in this work.

The space variant effect has been found to affect the lateral resolution performance in DH system [11-12]. However its influence on the axial performance has not been investigated. In this work, the influence of space variant on the axial error is investigated by both simulation and experiments. The results show that the space variant effect is an important contributor to the axial error. Due to its influence, objects are suggested to be placed on the optical axis and symmetrically with respect the optical axis for better axial accuracy.

2. The Analysis of Digital Holographic System Based on PSF

The PSF model of an arbitrary point $\delta(x-x_0)$ in DH system has been introduced in reference [10] by including the finite CCD size, pixel integration, sampling effect and reference wave and its conjugate according to diffraction theory [13]. It is presented as:

$$PSF(x_2)=\exp\left[-\frac{j\pi}{\lambda z}(x_2^2-x_0^2)\right]\times\left\{\left[\exp\left(-j2\pi\frac{x_0+\lambda z a}{2p}x_2\right)\times rect\left(\frac{x_2}{2p}\right)\right]\otimes\sin c\left(\frac{2D}{\lambda z}x_2\right)\otimes\delta(x_2-x_0)\right\} \quad (1)$$

where $\otimes$ denotes convolution. λ, z, a, 2D and $2p$ are the wavelength, the reconstruction distance, the carrier frequency introduced by reference wave, the CCD chip size and the pixel sensing size, respectively. x_2 is the coordinate of image plane. x_0 is the location of the point source $\delta(x-x_0)$ in the object plane. Due to the separable property of Fresnel transform, only one dimension case is considered and it can be extended to two dimensions readily.

In an ideal system, the image of an arbitrary point $\delta(x-x_0)$ at object plane is $\delta(x_2-x_0)$. However, due to the limitations in DH technique, the acquired reconstructed image becomes Eq. (1) instead of $\delta(x_2-x_0)$. Limitations result in not only an amplitude spread of PSF but also the associated phase error and therefore axial error. The axial error, rooting in three factors $\exp[-j2\pi(x_0+\lambda z a)/(2p)\times x_2]$, $\sin c[2D/(\lambda z)\times x_2]$ and $\exp[-j\pi/(\lambda z)\times(x_2^2-x_0^2)]$, is determined by the interaction of 2D, x_0, 2p and a. With different point position x0, the axial error differs. This character is the space variant effect of PSF in the axial error.

In practices, the specimens are objects with finite size rather than a point. For an object f(x) with size L, its reconstructed image is the weighted summation of the all the PSFs along the object size as

$$Rf(x_2)=\int_{L_1}^{L_2}A(x_0)PSF(x_2-x_0)dx_0 \quad (2)$$

where $A(x_0)$ is the amplitude at the point x_0. L2 and L1 satisfies that L2-L1=L. Due to the space variant effect of PSF, different

 ISSN 0097-966X/14/4502-0664-$1.00 © 2014 SID

placements of the object means the summations of PSFs at different sets of point positions x0. Therefore object placements associate with axial error performances. The simulation based on Eqs. (1) and (2) is performed in the investigation of the axial error in the following section.

3. Simulation Investigation of the Influence of Space Variant Effect on Axial Error

In this section, we investigate the impact of object displacement on axial error by simulation. The object used in simulation is a flat step with the OPD profile in Fig. 1(a). The step provides a 100 nm OPD between the step surface and the substrate. The step width in x and y directions are 1mm and 204.6 μm, respectively. In the simulation, the wavelength λ is 633 nm and the reconstruction distance z is 123 mm. Off-axis lens-less geometry is adopted. The CCD size, pixel size and carrier frequency are 2D=3.72 mm, 2p=T=4.65 μm and a=53.76×103 Hz.

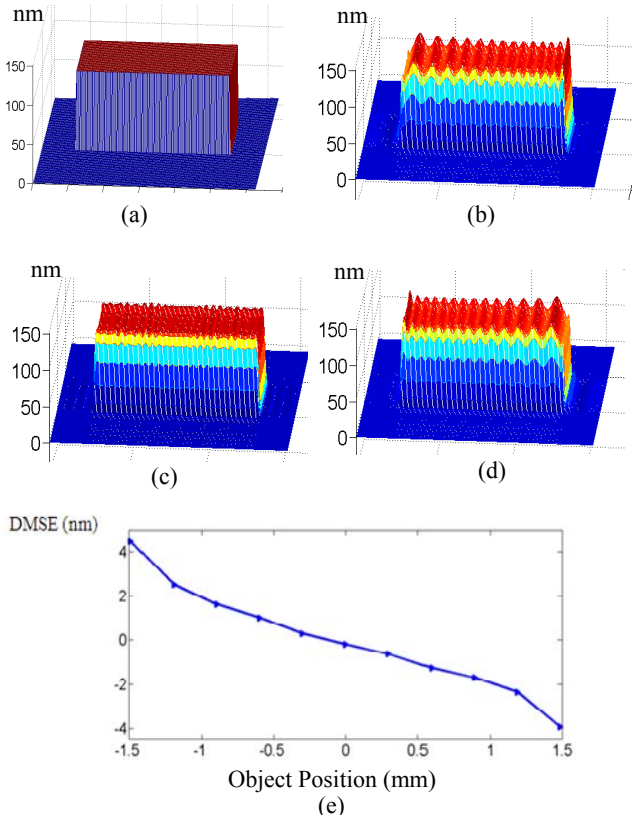

Figure 1. (a) The original object-a step of 100 nm height in simulation; (b) the reconstructed image at displacement -1.53 mm; (c) the reconstructed image at displacement 0; (d) the reconstructed image at displacement 1.53 mm; (e) Relationship between DMSE and the object displacement.

In holographic imaging, the optical axis passes through the middle point of the object/image plane and is perpendicular to the object/image plane. We define the placement where the object is symmetrically located with respect to the optical axis as displacement 0. The placements shifted left and right to the optical axis are defined as negative displacements and positive displacements, respectively. In the investigation, the reconstructed images are obtained by varying the object displacement.

The impact of object position on the OPD error is investigated by changing the object displacement from -1.488 mm to 1.488 mm at object plane with an interval of 0.2976 mm. Examples of the reconstructed OPD image of the object are shown by the blue dotted line in Figs. 1(b)-(d). The OPD error of the reconstructed image can be easily noticed. When the object is asymmetrically located with respect to the optical axis, the OPD error becomes asymmetrical as seen in Figs. 1(b) and 1(d). When the object is symmetrically located with respect to the optical axis, the OPD error is symmetrically distributed as seen in Fig. 1 (c). To identify the extent of asymmetry of the OPD error, we define the difference of the mean square error of the left side and the right side of the step surface (DMSE) as an index to investigate the relationship between the error asymmetry and the object displacement. Fig. 1 (e) shows the relationship between DMSE and the object displacement. It can be seen that larger object displacement with respect to the optical axis results in larger asymmetry of the OPD error.

This asymmetry of the OPD error roots in the space variant property of DH system. In the ideal system, the PSF of DH system $\delta(x_2-x_0)$ has zero phase error. In practice, The PSF is space variant as in Eq. (1) which has two factors related to phase error and x_0: $\exp[-j\pi/(\lambda z)\times(x_2^2-x_0^2)]$ and $\exp[-j2\pi\times(x_0+\lambda z a)/(2p)\times(x_2-x_0)]$. The former phase factor plays a major role in the phase error. Because its slope is about 103 times more sensitive than that of the second factor. The phase error of the PSF is larger at larger absolute value of x_0. Therefore positions further away from the optical axis suffer more severe phase error. When an object is asymmetrically placed with respect to the optical axis, longer side suffers larger OPD error in the reconstructed image. Hence the OPD error is asymmetrical in such case.

4. Experimental Results

In this part, the impact of object displacement on the axial error is experimentally examined. Seven holograms with G2E3 displacement ranging from -1.53 mm to 1.53 mm in a step of 0.51 mm are recorded. The OPD images of G2E3 are reconstructed at different displacements. Three of the seven holograms and the according OPD images are shown in Fig. 2 as an example. The changes in the axial errors at different displacements are easily noticed in the profile insets of Fig. 2 (e), (f) and (g), especially at edges. To quantify these changes, the DMSEs of G2E3 at different displacements are evaluated and shown in Fig. 3. The result shows that larger object displacement with respect to the optical axis results in larger asymmetry of the axial error. This result agrees with the one obtained in simulation part. Displacement from the optical axis causes asymmetry in the axial error. The change of the asymmetry of OPD error is in -9 nm to 9 nm range in experiment as shown in Fig. 3. Comparing to the magnitude of current axial error about tens of nanometers, the object displacement plays an important role in the axial error. Therefore the object is suggested to be placed symmetrically with respect to the optical axis for less and symmetrical axial error.

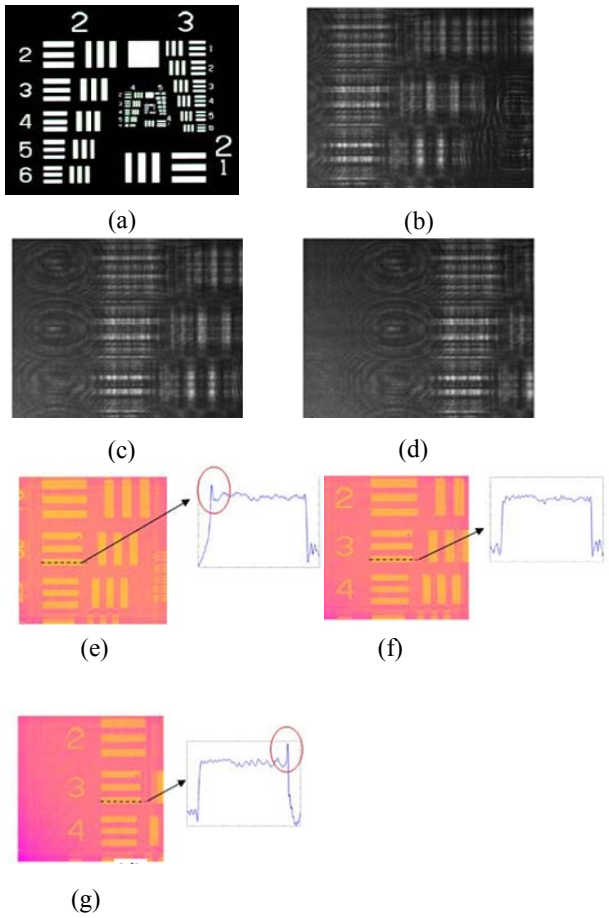

Figure 2. (a) USAF target; holograms with object displacements of (a) -1.53mm; (b) 0mm; (c) 1.53mm; the height images and profiles (insets) of G2E3 with object displacements of (d) -1.53mm; (e) 0mm; (f) 1.53mm; the 3D profile of G2E3 bar with object displacements of (g) -1.53mm; (h) 0mm; (i) 1.53mm.

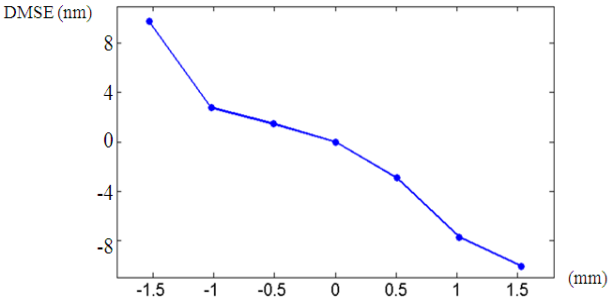

Figure 3. Relationship between the DMSE and the object displacement.

5. Conclusions

In this work, the influence of space variant effect on the axial imaging error in DH is investigated. It is demonstrated that the space variant effect not only affect to the lateral resolution but also the axial imaging performance in DH by both simulation an experiment. It is proved that different object placements result in different axial error performances. When the object is asymmetrically placed with respect to the optical axis, the axial error is asymmetrically distributed. The longer side presents more severe axial error than the shorter side, especially at the edge. This results in an axial error tilt along the object. Therefore a flat step will be measured as a tilt surface, which is obviously presented at the step edges. The measurement of the two edges with the same height of 100nm ended with a averaged height measurement difference of about 10nm at a displacement about 1.5 mm. Considering the current axial error magnitude in tens of nanometers, the space variant effect is therefore an important contributor to the axial error in DH technique. Therefore, the object is suggested to be placed on the optical axis and symmetrically for better axial imaging performance. The demonstration of the impact of space variant effect on the axial error in this work can be helpful for further investigation of axial error reduction and axial resolution improvement in future.

6. Acknowledgements

This work is sponsored by 973 Program (2013CB328804), National Natural Science Foundation of China (61307028), and Science & Technology Commission of Shanghai Municipality (13ZR1420000, 11JC1405300).

7. References

[1] U. Schnars and W. Juptner, “Direct recording of holograms by a CCD target and numerical reconstruction,” Applied Optics 33, 179-181 (1994).

[2] E. Cuche, F. Bevilacqua, and C. Depeursinge, “Digital holography for quantitative phase-contrast imaging,” Optics Letters 24, 291-293 (1999).

[3] N. Pandey and B. Hennelly, “Quantization noise and its reduction in lensless Fourier digital holography,” Applied Optics 50, B58-B70 (2011).

[4] D. Carl, B. Kemper, G. Wernicke, and G. von Bally, “Parameter-optimized digital holographic microscope for high-resolution living-cell analysis,” Applied Optics 43, 6536-6544 (2004).

[5] P. Marquet, B. Rappaz, P. J. Magistretti, E. Cuche, Y. Emery, T. Colomb, and C. Depeursinge, “Digital holographic microscopy: a noninvasive contrast imaging technique allowing quantitative visualization of living cells with subwavelength axial accuracy,” Optics Letters 30, 468-470 (2005).

[6] T. Colomb, E. Cuche, F. Charriere, J. Kuhn, N. Aspert, F. Montfort, P. Marquet, and C. Depeursinge, “Automatic procedure for aberration compensation in digital holographic microscopy and applications to specimen shape compensation,” Applied Optics 45, 851-863 (2006).

[7] B. Rappaz, P. Marquet, E. Cuche, Y. Emery, C. Depeursinge, and P. J. Magistretti, “Measurement of the integral refractive index and dynamic cell morphometry of living cells with digital holographic microscopy,” Optics Express 13, 9361-9373 (2005).

[8] F. Charriere, J. Kuhn, T. Colomb, F. Montfort, E. Cuche, Y. Emery, K. Weible, P. Marquet, and C. Depeursinge, “Characterization of microlenses by digital holographic microscopy,” Applied Optics 45, 829-835 (2006).

[9] C. J. Mann, L. F. Yu, C. M. Lo, and M. K. Kim, "High-resolution quantitative phase-contrast microscopy by digital holography," Optics Express 13, 8693-8698 (2005).

[10] Y. Hao and A. Asundi, "mpact of charge-coupled device size on axial measurement error in digital holographic system," Optics Letters 38, 1194-1196 (2013).

[11] D. P. Kelly, B. M. Hennelly, N. Pandey, T. J. Naughton, and W. T. Rhodes, "Resolution limits in practical digital holographic systems," Optical Engineering 48(2009).

[12] Y. Hao and A. Asundi, "Resolution Analysis of A Digital Holography System," Applied Optics 50, 11 (2011).

[13] J. W. Goodman, Introduction to Fourier Optics, 2nd ed. (McGRAW-HILL, 1996).